Macedonian Journal of Chemistry and Chemical Engineering, Vol. **43**, No. 2, pp. 257–270 (2024)

MJCCA9 – 911

ISSN 1857-5552
e-ISSN 1857-5625

Received: April 10, 2024
Accepted: November 5, 2024

DOI: 10.20450/mjcce.2024.2867
Original scientific paper

PREPARATION, CHARACTERIZATION, AND USE OF TRIMETHOXY[3-(METHYLAMINO)PROPYL]SILANE FUNCTIONALIZED SBA-15 FOR CONGO RED ADSORPTION

Mukaddes Can, Suzan Albayati, Hani Zeidan, Mustafa Esen Marti*

Department of Chemical Engineering, Konya Technical University, Konya, Turkey
memarti@ktun.edu.tr & mustafaesenmarti@gmail.com

Mesoporous materials have a broad range of applications in industry, and one of which is their potential use in adsorptive separations. This research investigates the use of a secondary amine-functionalized SBA-15 for the separation of a diazo dye, Congo Red (CR), from aqueous solutions. The synthesized SBA-15 was modified with trimethoxy[3-(methylamino)propyl] silane by a post-grafting method. The produced material was characterized using X-ray diffraction, N_2 physisorption, scanning electron microscopy, and transmission electron microscopy. The hexagonal mesostructure was preserved after functionalization; however, the specific surface area, pore diameter, and total pore volume of SBA-15 silica decreased. The adsorption of the diazo dye reached equilibrium by 50 minutes, and the data followed pseudo-second-order kinetics. While the yield increased with rising dosage and temperature, it decreased with CR concentration. The maximum adsorption capacity of functionalized SBA-15 (F-SBA-15) for CR uptake was found to be 211.07 mg/g. Thermodynamic data and parameters indicated the potential combination of physical and chemical interactions occurring during the adsorption process. The separation was endothermic and non-spontaneous; the equilibrium data fitted to the Freundlich adsorption isotherm at all tested temperatures. This study demonstrates that the secondary amine-functionalized SBA-15 can be used for the elimination of a toxic anionic diazo dye from aqueous solutions.

Keywords: SBA-15; isotherm; kinetics; thermodynamics; trimethoxy[3-(methylamino)propyl]silane

ПОДГОТОВКА, КАРАКТЕРИЗАЦИЈА И УПОТРЕБА НА SBA-15 ФУНКЦИОНАЛИЗИРАН СО ТРИМЕТОКСИ[3-(МЕТИЛАМИНО)ПРОПИЛ]СИЛАН ЗА АДСОРБЦИЈА НА КОНГО ЦРВЕНО

Мезопорозните материјали имаат широк опсег на примена во индустријата, а една од нив е нивната потенцијална употреба во атсорптивни сепарации. Ова истражување ја испитува употребата на SBA-15 функционализиран со секундарен амин за издвојување на диазо-бојата конго црвено (CR) од водни раствори. Синтетизираниот SBA-15 беше модифициран со триметокси[3-(метиламино)пропил]силан со метод на пост-калемење. Произведениот материјал беше карактеризиран со помош на дифракција на рендгенски зраци, физисорпција на N_2, скенирачка електронска микроскопија и трансмисиона електронска микроскопија. Шестоаголната мезоструктура беше зачувана по функционализацијата; сепак, специфичната површина, дијаметарот на порите и вкупниот волумен на порите на силициум диоксид SBA-15 се намалија. Атсорпцијата на диазо-бојата достигна рамнотежа за 50 минути, при што следеше кинетика од псевдо-втор ред. Додека приносот со зголемувањето на дозата и температурата се зголемува, со концентрацијата на CR се намалува. Утврдено е дека максималниот капацитет на атсорпција на функционализираниот SBA-15 (F-SBA-15) за впивање на CR е 211,07 mg/g. Термодинамичките податоци и параметри ја покажаа потенцијалната комбинација на физички и хемиски интеракции што се случуваат за време на процесот на атсорпција. Раздвојувањето беше ендотермно и неспонтано; податоците за рамнотежата ја следеа изотермата на атсорпција на Фројндлих на сите тестирани температури. Оваа студија покажува дека SBA-15 функционализиран со секундарниот амин може да се користи за елиминација на токсичната анјонска диазо-боја од водни раствори.

Клучни зборови: SBA-15; изотерма; кинетика; термодинамика; триметокси[3-(метиламино)пропил]силан

1. INTRODUCTION

Santa Barbara Amorphous-15 (SBA-15) has significant advantages due to its distinctive properties, including small crystallite size of primary units, thick framework walls, hydrothermal and mechanical stability, and unique pore structure.[1] Furthermore, its high internal surface area enables its use in various applications, including adsorption and catalysis.[2] Several researchers have developed mesoporous silica materials as adsorbents for environmental remediation applications.[3] The modification of the SBA-15 surface with different functional groups creates active sites, enhancing its adsorption capabilities.[1,4] Various studies in the literature have confirmed this tendency for the separation of heavy metals,[5–8] synthetic dyes,[9,10] and other pollutants.[11,12]

Currently, due to accelerated population growth and urbanization, environmental contamination problems caused by industrial effluent is increasing and posing significant challenges in water resource management.[13] Industries such as textile, painting, printing, and tanning generate wastewater containing several types of toxic synthetic dyes.[14,15] The effluents require remediation prior to discharge into the environment.[16] Even minimal doses of dyes in water make it unsafe for living organisms.[17] Many techniques, including coagulation, ultrafiltration, photocatalytic degradation, and ozonation, have been examined for the remediation of toxic pollutants. Adsorption is recognized as a highly effective method for wastewater treatment because of its efficiency, simplicity, selectivity, cost-effectiveness, and high recyclability.[18]

Recently, SBA-15 modified with several functional groups was evaluated for its efficiency in removing colorants from aqueous-based media. Melamine-based dendrimer amine-functionalized SBA-15 was used to treat water containing 10 mg/l methylene blue (MB). A removal efficiency of 98 % was obtained at pH 10, with a 3 g/l adsorbent dose at 25 °C, which were determined to be optimum conditions.[19] The performance of polypyrrole-modified SBA-15 for the removal of MB and methyl orange was assessed. The surface area decreased by ~37.5 % following modification, and the maximum adsorption capacities (q_{max}) for each dye were 58.8 and 41.7 mg/g, respectively.[20] In a following study, MB removal efficiency was significantly improved by modifying SBA-15 with calcium alginate/amines.[21] SBA-15 modified with lignosulfonate/amino groups exhibited a maximum uptake capacity of 62.9 mg/g for the same colorant.[22] The capacity of SBA-15 to remove Reactive Blue 15, an anionic dye, was almost zero; however, it increased to 25.7 mg/g after the incorporation of bridging polysilsesquioxane into the mesoporous material.[23] The composite obtained from a single-step modification of SBA-15 with iron and γ-chitosan was tested for the removal of MB. The maximum performance (176.70 mg/g) of the synthesized adsorbent was achieved at pH 9.[24] The functionalization of SBA-15 with a tertiary amine facilitated the elimination of Congo Red (CR), with a maximum capacity (q_{max}) of 186.4 mg/g.[10] The study investigated the elimination of three anionic dyes, namely, Acid Blue, Direct Black ANBN, and Direct Yellow 12 from aqueous solution with chitosan-SBA-15-NH_2, achieving maximum adsorption capacities of 43.5, 200, and 40 mg/g, respectively.[9]

This study tested the trimethoxy[3-methyl–amino)propyl]silane-functionalized SBA-15 for the removal of a synthetic dye from aqueous-based solutions. Numerous industries, from paper to cosmetics, use Congo Red (CR), a carcinogenic diazo dye that requires an efficient method for removal from aqueous-based effluents.[25] Accordingly, we synthesized and modified SBA-15 using a secondary amine and tested it as an adsorbent during the separation of a toxic diazo dye, CR, from model aqueous solutions. Prior to the adsorption tests, the adsorbent material was characterized by several techniques. The impacts of process variables such as contact time, dye concentration, temperature, and adsorbent dosage were examined. Moreover, the data were interpreted using several kinetic and isotherm models, and thermodynamic constants were calculated.

2. EXPERIMENTAL

2.1. *Materials*

Pluronic P 123 (triblock co-polymer, $PEO_{20}PPO_{70}PEO_{20}$, 96 %) and tetraethyl orthosilicate (TEOS, > 99.99 %) were supplied from Sigma Aldrich and used with HCl (Isolab, ≥ 37%) in the synthesis of SBA-15. Trimethoxy[3-(methylamino) propyl] silane (> 95 %) and toluene (≥ 99 %) were used to functionalize SBA-15 and were obtained from TCI and Merck, respectively. Congo Red (CR, ≥ 75 % dye basis) was provided by Merck Co. A Millipore Direct-Q 3V system was utilized to provide ultra-high purity (UHP) water. Dye solutions were prepared by dissolving CR in UHP water. Analytical-grade chemicals were employed in the trials with pretreatment. The chemicals utilized in this work are listed in Table 1.

T a b l e 1

The chemicals utilized in the present study

Compound	Source	CAS no.	Purity (%)
Pluronic P 123	Sigma Aldrich	9003-11-6	96
Tetraethyl orthosilicate	Sigma Aldrich	78-10-4	> 99.99
Hydrochloric acid	Isolab	7647-01-0	≥ 37
Trimethoxy[3-(methylamino)propyl]silane	TCI	3069-25-8	≥ 95
Toluene	Merck	108-88-3	≥ 99
Congo Red	Merck	573-58-0	≥ 75

2.2. *Synthesis of amine-functionalized SBA-15 (F-SBA-15)*

SBA-15 was synthesized as described previously.[26] At ambient temperature, 4 g of Pluronic P 123 was added to 150 ml of 1.6 M HCl and mixed for an hour. Following addition of 9 ml of TEOS, the mixture was stirred at 35 – 40 °C for 20 hours. After this, the solution was heated and maintained at 85 °C for 24 hours, then filtered. The product was obtained and then calcined in air flow at 500 °C for 5 hours.

To make the amine-functionalized or modified SBA-15 (F-SBA-15), 3.8 g of trimethoxy[3-(methylamino)propyl]silane was mixed with a suspension containing 2 g of SBA-15 in 100 ml of toluene to modify the mesoporous material. Functionalization was conducted at 65 °C under reflux. The mixture was agitated for 12 hours and then subjected to filtration and washing with toluene to remove any residual amine. This step was repeated a minimum of five times using a Nutsch filter with a porosity of #4 under vacuum.

2.3. *Characterization*

The synthesized samples (SBA-15 and F-SBA-15) were characterized via small-angle X-ray scattering (SAXS), wide-angle X-ray diffraction (WXRD), N_2 physisorption, scanning electron microscopy (SEM, Zeiss), and transmission electron microscopy (TEM, JEOL JEM-2100). XRD data were obtained on a Rigaku-Miniflex diffractometer utilizing Cu-K_α radiation (λ = 1.5405 Å) at a voltage of 30 kV and a current of 15 mA. Small-angle XRD patterns were obtained within the 2θ range of 0.5–5° with 0.005° steps and 0.2° data collection per minute, while WXRD patterns were obtained within the 2θ range of 5.0–75.0° with 0.05° steps and 1° data collection per minute. A Micromeritics ASAP 2000 volumetric apparatus was employed to determine the surface area and pore characteristics of the synthesized silica samples using N_2 adsorption at 77 K. Prior to the analysis, the samples were subjected to an 8-hour outgassing process at 363 K in a vacuum. The particle morphology of the produced adsorbent materials was assessed by SEM. The mesoporous structure of the synthesized adsorbents was examined with a JEOL JEM-2100 TEM instrument.

2.4. *Adsorption procedure*

In a previous study, the highest efficiency for CR removal using amine-modified SBA-15 was achieved at the original pH (8.8) of the model solution.[10] In addition, 98 % efficiency was obtained in the remediation of Brilliant Red by chitosan-SBA-15 at pH 7.0 in 80 minutes.[27] Therefore, all adsorption experiments were performed at the original pH values of the model solutions, ranging from pH 7.9 to 8.2, with a standard uncertainty of ± 0.1.

Aqueous and solid phases were mixed in Erlenmeyer flasks. To separate the phases, the mixtures were centrifuged at 4600 *g* for two minutes. Spectrophotometric determination of CR in the aqueous phase was conducted on a Jenway 7205 at the maximum absorbance for CR (λ_{max} of 497 nm). Adsorption yield (Y, %) and uptake or adsorption capacity (q_e) were computed by Eqs. 1 and 2, respectively; C_o and C_e are the initial and equilibrium concentrations (mg/l) of CR, m is the mass (g) of adsorbent (F-SBA-15), and V (l) is the volume of the aqueous solution.

$$Y(\%) = \left(\frac{C_o - C_e}{C_o}\right) \times 100 \quad (1)$$

$$q_e = \left(\frac{C_o - C_e}{m}\right) \times V \quad (2)$$

Kinetic trials were conducted by contacting the mesoporous adsorbent (2.5 mg of F-SBA-15) with 10 ml (0.25 g/l dose) of CR solution (50 mg/l) in a 50 ml Erlenmeyer flask at 303 K. The samples were withdrawn at various intervals, centrifuged, and the supernatants analyzed for CR concentration. The effect of temperature was probed in the range of 303–323 K. Thermodynamic constants, including changes in Gibbs free energy ($\Delta G°$,

kJ/mol), enthalpy (Δ*H*°, kJ/mol), and entropy (Δ*S*°, J/mol·K) were computed employing Eqs. 3 – 5.

$$\Delta G^{o} = -R \times T \times \ln K_{L} \quad (3)$$

$$K_{L} = \frac{q_e}{Ce} \quad (4)$$

$$\ln (K_{L}) = -\frac{\Delta H^{o}}{R \times T} + \frac{\Delta S^{o}}{R} \quad (5)$$

In these equations, R is the gas constant (8.314 J/mol·K), T is temperature (K), and K_L is the Langmuir equilibrium constant (l/mg). C_e and q_e are the dye concentration (mg/l) in the solution and adsorption capacity (mg/g) at equilibrium, respectively. To observe the effect of F-SBA-15 dosage and CR concentration, trials were conducted at 0.25–0.75 g/l and 25–75 mg/l, respectively.

3. RESULTS AND DISCUSSION

3.1. *Characterization*

Figure 1a displays the XRD patterns of SBA-15 and F-SBA-15. Verification of their mesoporous structures was conducted through small-angle XRD scanning from 0.5° to 5° (Fig. 1a). The low-angle XRD pattern of SBA-15 has a pronounced peak at 2θ of 0.95°, with two additional weaker peaks at 1.6° and 1.8°. These peaks are assigned to the (100), (110), and (200) planes in the low angle range and characterize the highly ordered SBA-15 with hexa–gonal p6mm structure.[28-31] It was observed that F-SBA-15 also exhibits an intense (100) peak and weaker (110) and (200) peaks, according to its low-angle XRD spectra. This indicates that modification with trimethoxy[3-(methylamino)propyl]silane groups does not disrupt the mesoporous structure of pure SBA-15. However, compared to pure SBA-15, the relative intensities of the characteristic diffraction peaks decreased due to the incorporation of organic components into the pore channels. This suggests that functionalization of SBA-15 results in decreased mesopore assembly.[32-34] Figure 1b depicts the wide-angle XRD pattern of SBA-15 in the scanning range 10° to 80°. As shown, the XRD pattern of SBA-15 displays a broad peak at around 23°, confirming the amorphous nature of the SBA-15.[35–37]

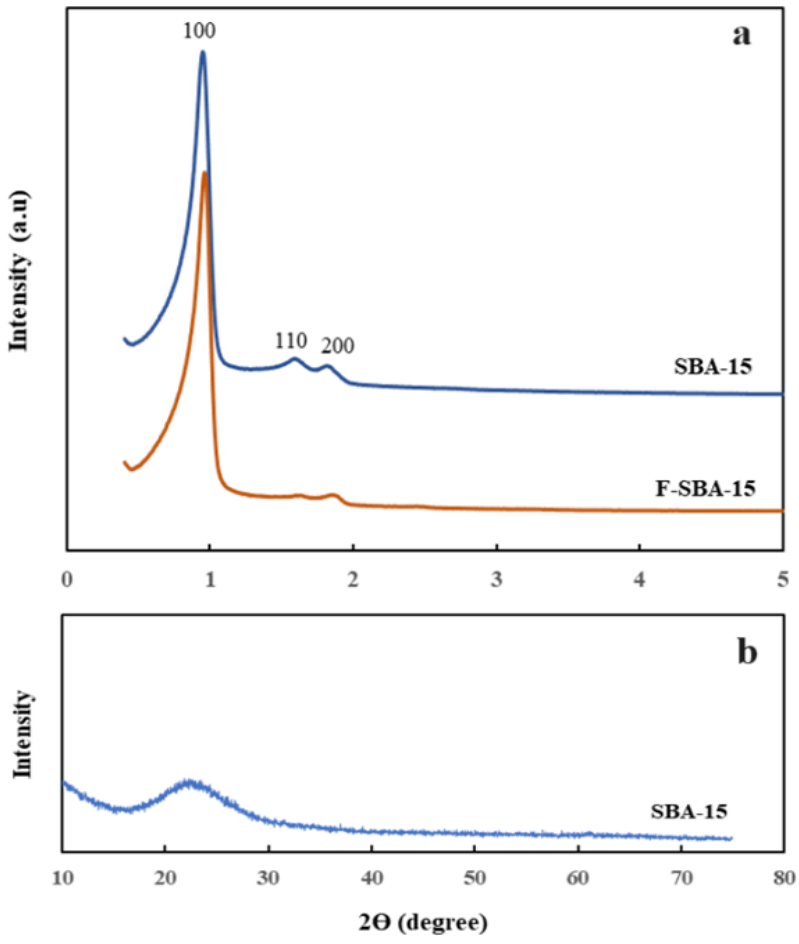

Fig. 1. (a) Small-angle XRD patterns of pure SBA-15 and F-SBA-15. (b) Wide-angle XRD pattern of SBA-15

The N_2 adsorption-desorption isotherms were conducted at 77 K to examine the porous structure and textural parameters, such as the surface area (S_{BET}, m^2/g), pore volume (V_t, cm^3/g), and pore diameter (D_P, nm) of SBA-15 and F-SBA-15. Figure 2 reveals that the samples displayed a type IV isotherm with an H1-type hysteresis loop, based on the IUPAC classification.[38] This observation demonstrates the characteristics of a mesoporous substance with elongated cylindrical channels and homogenous pores.[39] Figure 2 clearly shows that SBA-15 exhibits a significant rise in adsorption when the relative pressure (P/P_o) ratio is between 0.6 and 0.8. This suggests that SBA-15 has substantial mesopores and a narrow variation of pore sizes.[33,34] In the case of F-SBA-15, the type IV isotherm with an H1 hysteresis was retained. However, the functionalization of SBA-15 resulted in a decrease in the amount of adsorbed nitrogen, according to the Brunauer-Emmett-Teller (BET) analysis.

Additionally, the isotherm inflection point shifts to a lower P/P_o ratio, indicating that incorporation of amino-silanes in SBA-15 leads to a decrease in pore size.[20,40,41] A summary of textural parameters obtained by N_2 adsorption/desorption is given in Table 2.

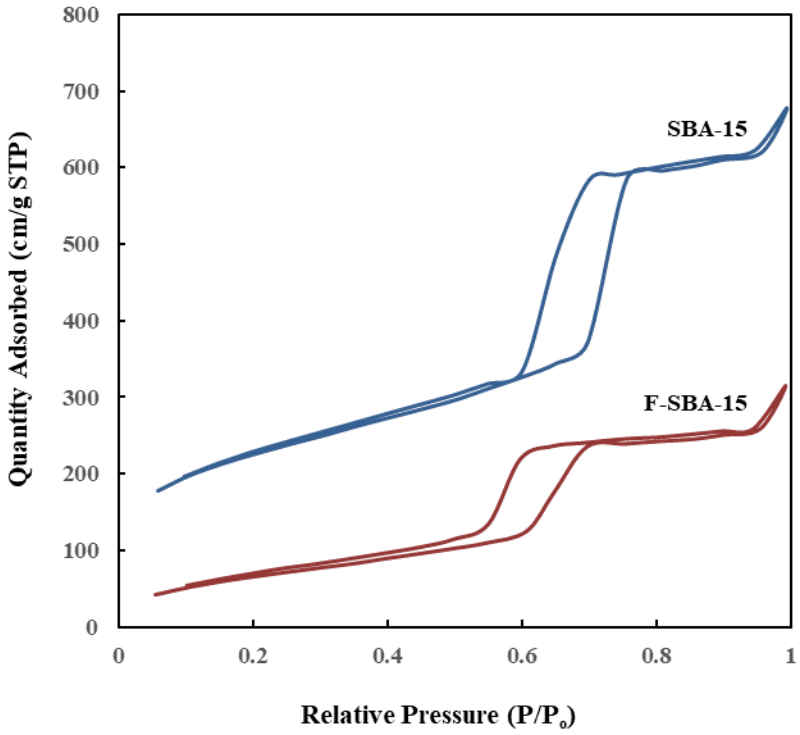

Fig. 2. N_2 adsorption-desorption isotherms for pure SBA-15 and F-SBA-15

T a b l e 2

Textural features of SBA-15 and F-SBA-15 determined by N_2 adsorption

Material	S_{BET} (m^2/g)	V_t (cm^3/g)	D_p (nm)
SBA-15	789.5	0.98	7.86
F-SBA-15	252.7	0.53	5.65

The morphology and mesoporous structure of pure SBA-15 and F-SBA-15 were studied using SEM and TEM. The SEM images show that pure SBA-15 contains rod-shaped nanoparticles, and the SBA-15 nanofibers have a relatively uniform hexagonal structure (Fig. 3a).[42–45] After amine functionalization, more agglomerated particles were observed that are attributable to changes in the symmetry of hexagonal mesopores after modification (Fig. 3b). These findings are in line with the outcomes of small-angle XRD and N_2 adsorption-desorption analyses, indicating that the ordering and hexagonal symmetry of the mesostructure decreased after functionalization.[38,44] The mesostruc-

ture of the modified SBA-15 sample was examined using TEM. Figure 4 clearly verifies that F-SBA-15 retains the characteristic two-dimensional hexagonal structure commonly observed in SBA-15. After functionalization with amine groups, the hexagonal mesostructure is well-maintained, clearly indicating that the surface modification did not destroy the mesostructure.[39,45,46] The results are consistent with the corresponding N_2 sorption results in Figure 2.

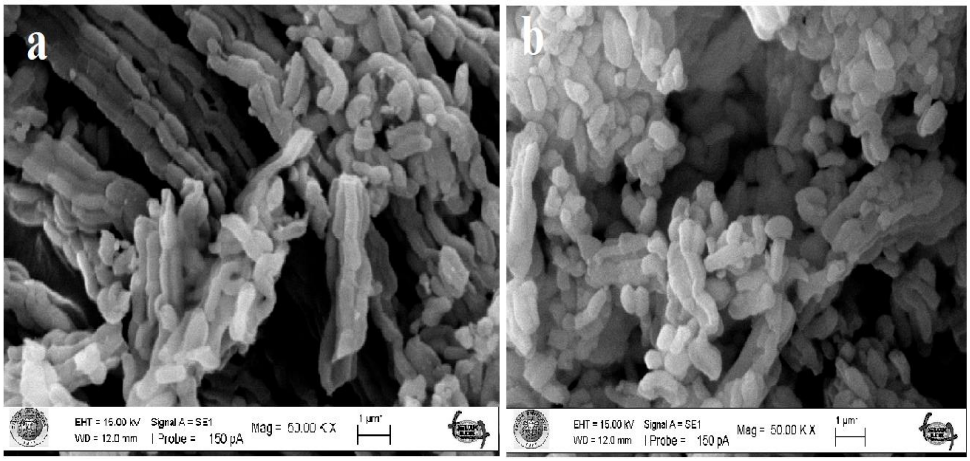

Fig. 3. SEM images of (a) pure SBA-15 and (b) F-SBA-15

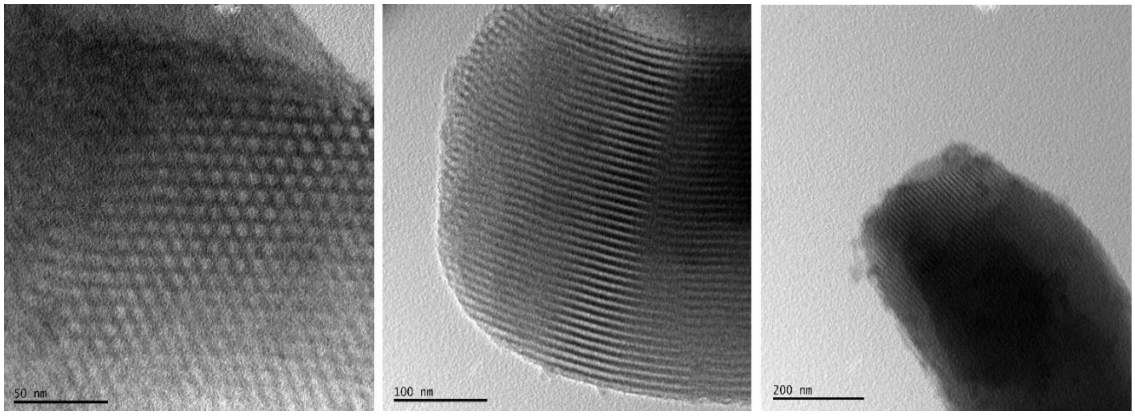

Fig. 4. TEM images of F-SBA-15 with different magnifications

3.2. *Kinetics*

Kinetic data examining the effect of contact time on CR uptake are depicted in Figure 5. Initially, the adsorption available sites on the surface were vacant and accessible for CR uptake. Therefore, the process rate was very fast in the first 20 min. Over time, the rate slowed as these sites became fully occupied due to diffusion of CR molecules on the porous F-SBA-15 adsorbent.[47] According to the data, the adsorption process reached equilibrium by 50 min. Hence, solid and liquid phases were brought into contact for about one hour in all subsequent experiments.

To investigate the possible mechanism controlling the rate of the removal process, pseudo-first-order (PFO) and pseudo-second-order (PSO) models were applied to the kinetic data.[48,49] In their expressions, k_1 (1/min) is the rate constant of PFO kinetic model, while k_2 (g/mg·min) is that of PSO kinetic model. In addition, the Elovich kinetic model, with the constants of α (initial adsorption rate, mg/g·min) and β (desorption constant, g/mg), and the intraparticle diffusion (ID) model were used to elucidate the data.[50,51] Expressions for these models are represented in Table S1. Figure 6 and Table 3 demonstrate that the PSO kinetics yielded the highest determination coefficient (R^2, 0.999), indicating that it is the most appropriate model for interpreting the data. In the kinetic graphs, t is time (min), while q_t (mg/g) is the amount of CR adsorbed per gram of adsorbent at time t. The uptake capacity under the studied conditions was found to

be 142.9 mg/g, which was essentially identical to the experimentally determined value (q_e = 142.3 mg/g). The R^2 values obtained with the PFO and Elovich kinetic models were comparatively low, suggesting chemical or physiochemical interactions between dye molecules and the adsorbent.[52] The first stage of the process appears to involve chemical adsorption, and over time, the surface sites that have the ability to interact with dye molecules become saturated. As a result, physical adsorption becomes dominant, and electrostatic repulsion occurs until equilibrium is reached.[53] The values of the boundary layer diffusion effect (I, mg/g) and ID rate constant (K_{id}) were calculated from the intercept and slope of the linear plot of q_t vs. $t^{0.5}$, respectively (Fig. 7 and Table 4). The line did not intersect the origin; hence, it can be assumed that the ID was not the only rate-controlling step for the removal of CR by F-SBA-15. It is clear from Figures 5 and 7 that the adsorption process does not occur in a single step, but rather involves the transfer of CR molecules from the bulk phase to the surface of F-SBA-15. Then, CR ions diffuse into the pores and reach a state of saturation at equilibrium.[18]

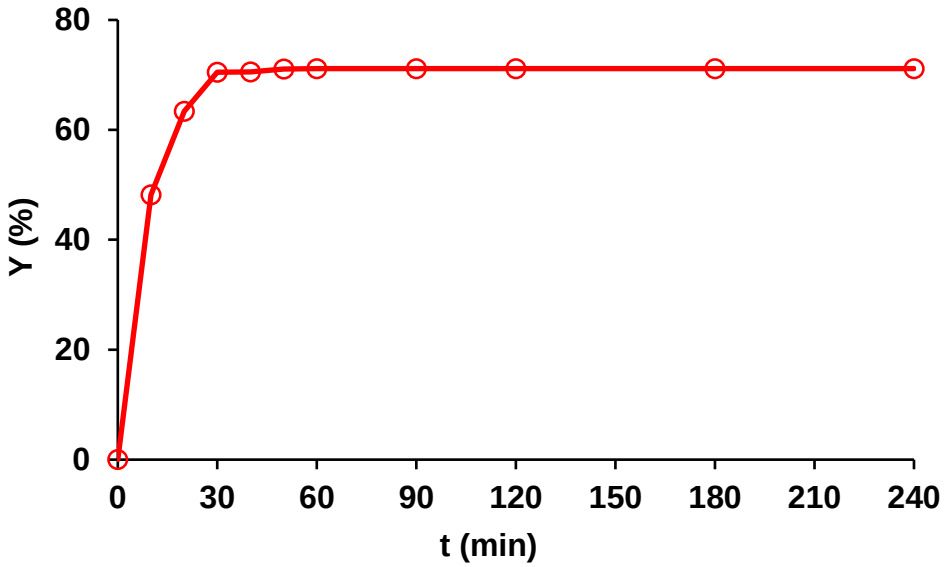

Fig. 5. Impact of contact time on CR uptake onto F-SBA-15 ([CR]$_o$: 50 mg/l; pH: 8.1; Dosage: 0.25 g/l; Temp.: 303 K)

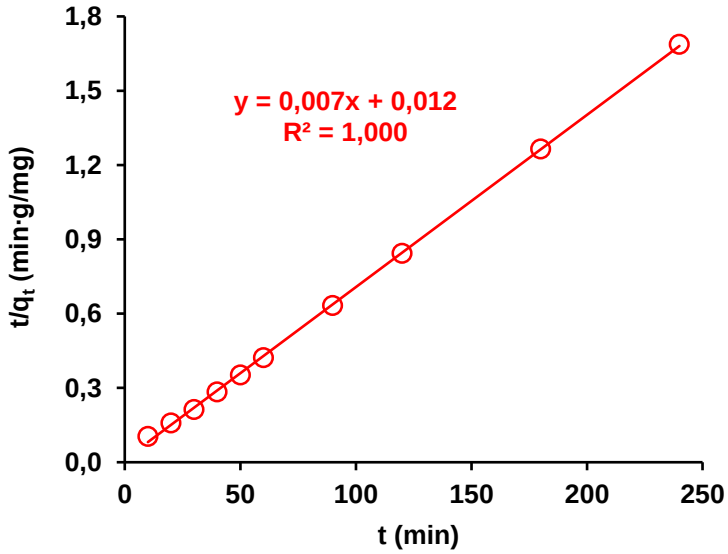

Fig. 6. Graph of the PSO model for CR uptake onto F-SBA-15 ([CR]$_o$: 50 mg/l; Dosage: 0.25 g/l; Temp.: 303 K)

Table 3

The constants and R^2 values obtained in kinetic analysis of data for CR uptake onto F-SBA-15. ([CR]$_o$: 50 mg/l; pH: 8.1; Dosage: 0.25 g/l; Temp.: 303 K)

T (K)	$q_{e,exp}$ (mg/g)	Pseudo-first-order			Pseudo-second-order			Elovich		
		k_1 (1/min)	$q_{e,cal}$ (mg/g)	R^2	k_2 (g/mg·min)	$q_{e,cal}$ (mg/g)	R^2	α (mg/g·min)	β (g/mg)	R^2
303	142.3	0.139	182.5	0.954	0.004	142.9	***1.000***	146.5	19.368	0.682

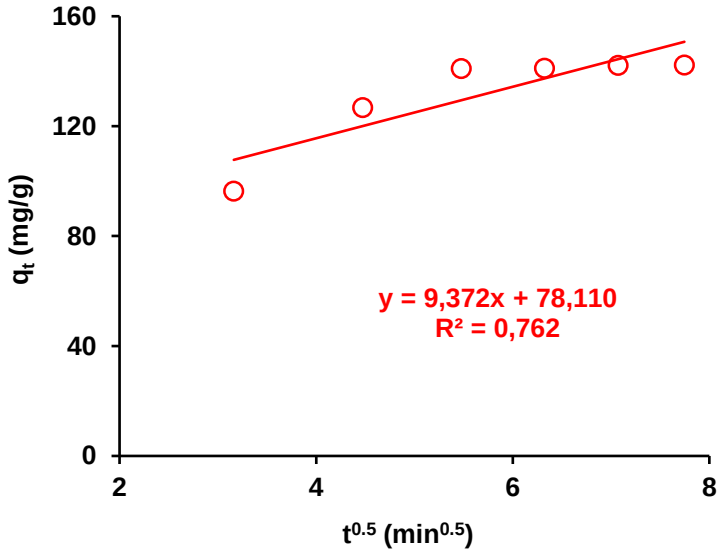

Fig. 7. The plot of ID model for CR uptake onto F-SBA-15 ([CR]$_o$: 50 mg/l; pH:8.1; Dosage: 2.5 g/l; Temp.: 303 K)

Table 4

The constants and R^2 values obtained with ID model for CR uptake onto F-SBA-15 ([CR]$_o$: 50 mg/l; pH: 8.1; Dosage: 0.25 g/l; Temp.: 303 K)

T (K)	K_{id} (mg/g·min$^{0.5}$)	I (mg/g)	R^2
303	9.37	78.11	0.762

3.3. *Thermodynamics*

The experiments for the adsorption of CR on F-SBA-15 were conducted at 303, 313, and 323 K (Fig. 8a). It can be seen that the adsorption yields are higher at elevated temperatures. This is due to the increasing molecular motion at higher temperatures, which allows molecules to enter the pores more easily. The results show the endothermic character of the process, which is consistent with earlier studies.[10] The data were used to determine the thermodynamic parameters. The positive Gibbs free energy ($\Delta G°$) confirms the non-spontaneous nature of the process. $\Delta H°$ and $\Delta S°$ were computed from the slope and intercept of the plots of ln(K_L) versus 1/T (Fig. 8b). The positive values of $\Delta H°$ and $\Delta S°$ signify that the adsorption process is endothermic and leads to an increase in disorder at the solid-liquid interface, respectively (Table 5). The magnitudes of the thermodynamic parameters revealed the possibility of physisorption or the combined influences of physical and chemical forces in the process.[54,55]

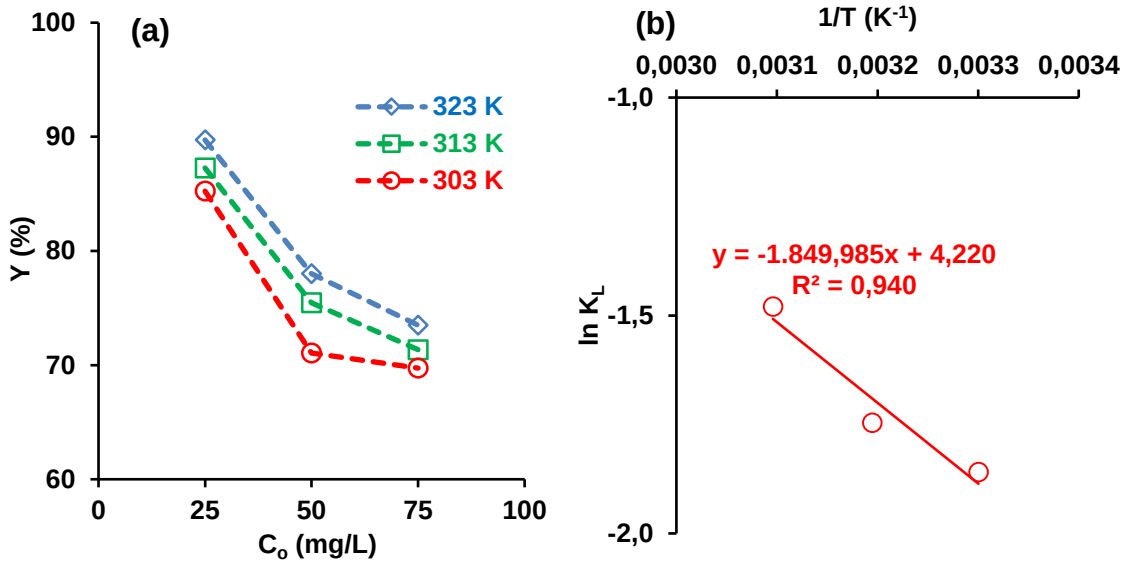

Fig. 8. (a) Temperature effect and (b) graph of ln K_L vs. 1/T for CR uptake using F-SBA-15 ([CR]$_o$: 25–75 mg/l; pH: 7.9–8.2; Dosage: 2.5 g/l; Temp.: 303 – 323 K)

T a b l e 5

Calculated thermodynamic constants for CR uptake onto F-SBA-15 ([CR]$_o$: 25 – 75 mg/l; pH: 7.9 – 8.2; Dosage: 0.25 g/l; Temp.: 303 – 323 K)

T (K)	$\Delta G°$ (kJ/mol)	$\Delta H°$ (kJ/mol)	$\Delta S°$ (J/mol·K)	R^2
303	4.68 ± 0.05			
313	4.54 ± 0.05	15.38 ± 0.16	35.08 ± 0.35	0.940
323	3.97 ± 0.04			

3.4. *Initial CR concentration and F-SBA-15 dosage*

It has previously been shown that pure SBA-15 cannot adsorb synthetic dyes and that adsorption yields were significantly lower without modification with an appropriate functional group.[10,23] Figure 9 illustrates the impact of the initial CR concentration and the dose of F-SBA-15 on the capacity and yield of adsorption. Depending on CR concentration, the initial pH varied between 7.9–8.2. The data illustrate that adsorption efficiency significantly decreased with a higher CR concentration and increased with a higher F-SBA-15 dosage (Fig. 9 and Table S2); however, this trend was reversed for adsorption capacity. The yield increased with the amount of F-SBA-15 due to the enhanced surface area, but it decreased with higher CR concentration, since the ratio of available binding sites to solute molecules in the medium decreased.[56-58] Within the tested parameter range, the maximum uptake capacity and yield were calculated to be 211.1 mg/g (Fig. 9a) and 92.1 % (Fig. 9b), respectively.

Table 6 shows that the maximum uptake capacity achieved with F-SBA-15 in this study is within the range of values obtained using various mesoporous adsorbents during the remediation of CR.[10,30,58-63] The adsorption process of CR on F-SBA-15 involves the formation of hydrogen bonds between the amino groups of the dye molecules and the nitrogen of the secondary amine on the surface of SBA-15. In addition, electrostatic attraction between the anionic dye and the protonated amine may also play an important role in the process.[63,64]

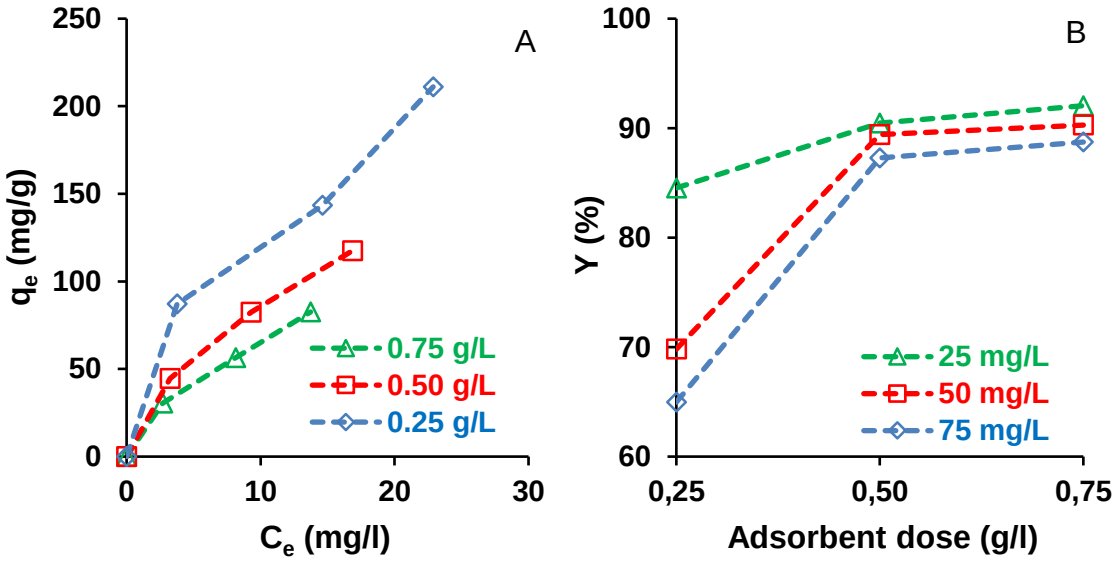

Fig. 9. Impact of F-SBA-15 dose and CR concentration on the process performance ([CR]$_o$: 25–75 mg/l; pH: 7.9–8.2; Dosage: 0.25–0.75 g/l; Temp.: 303 K)

T a b l e 6

Maximum CR uptake capacities obtained by different mesoporous silica adsorbents

Adsorbents	q_{max} (mg/g)	Reference
F-SBA-15	211.1	This work
SBA-15	87.3	(Chaudhuri et al., 2015)[60]
AF-SBA-15	186.4	(Zeidan et al., 2023)[10]
SBA-15 -NH_2	231	(Lu et al., 2005)[58]
MCM -48-NH_2	66.5	(Sholehah et al., 2021)[63]
MCM-48	185.2	(Abdelkader et al., 2016)[61]
P,P-bis (2-oxooxazolidin-3-yl)-*N*-(3-(triethoxysilyl)propyl)phosphinic amide functionalized SBA-15	518.1	(Zhang et al., 2019)[30]
Zeolite A-modified hexadecyltrimethylammonium bromide	21.1	(Khalaf et al., 2021)[62]
Acid activated red mud	7.1	(Xia et al., 2011)[59]

3.5. *Isotherm models*

Adsorption isotherm models are very useful for interpreting the affinity between an adsorbent and adsorbate at liquid-solid interfaces. The type of adsorption (chemical or physical), surface feature, and capacity of the sorbent material can be estimated using these models. Langmuir, Freundlich, and Temkin are the most commonly used isotherms for modeling liquid-solid adsorption processes.[65–67] The equations of these models and their linearized expressions are given in Table S3. Table 7 shows that the R^2 values with the Freundlich isotherm model were slightly higher than those obtained with the other two models (Fig. 10), indicating the multilayer structure of CR on the heterogeneous surface of F-SBA-15. It was found that the adsorption capacity of Freundlich isotherm model (K_F, l/mg) increased with increasing temperature, and adsorption was achievable at higher temperatures. The values of adsorption intensity (n) lie between 1 and 10, indicating that the adsorption process is favorable.[68] In addition, the maximum experimental adsorption capacities (206.3, 213.2, and 218.1 mg/g) were in agreement with the values of the theoretical maximum (Q_{max}, mg/g), calculated according to the Langmuir isotherm. They were found to be 232.6, 243.9, and 243.9 mg/g at 303, 313, and 323 K, respectively (Table 7). Furthermore, the values of the dimensionless separation factor, R_L, of the Langmuir isotherm were calculated to be in the range 0.01–0.20 (Table 7), indicating the favorable nature of the adsorption process.[69] In the Temkin isotherm model equation, B

(J/mol) and K_T (l/mg) are the Temkin equilibrium binding constant and the constant related to the adsorption heat, respectively. The relatively high R^2 values of the Temkin isotherm suggest a uniform distribution of the binding energy up to the maximum value.[70]

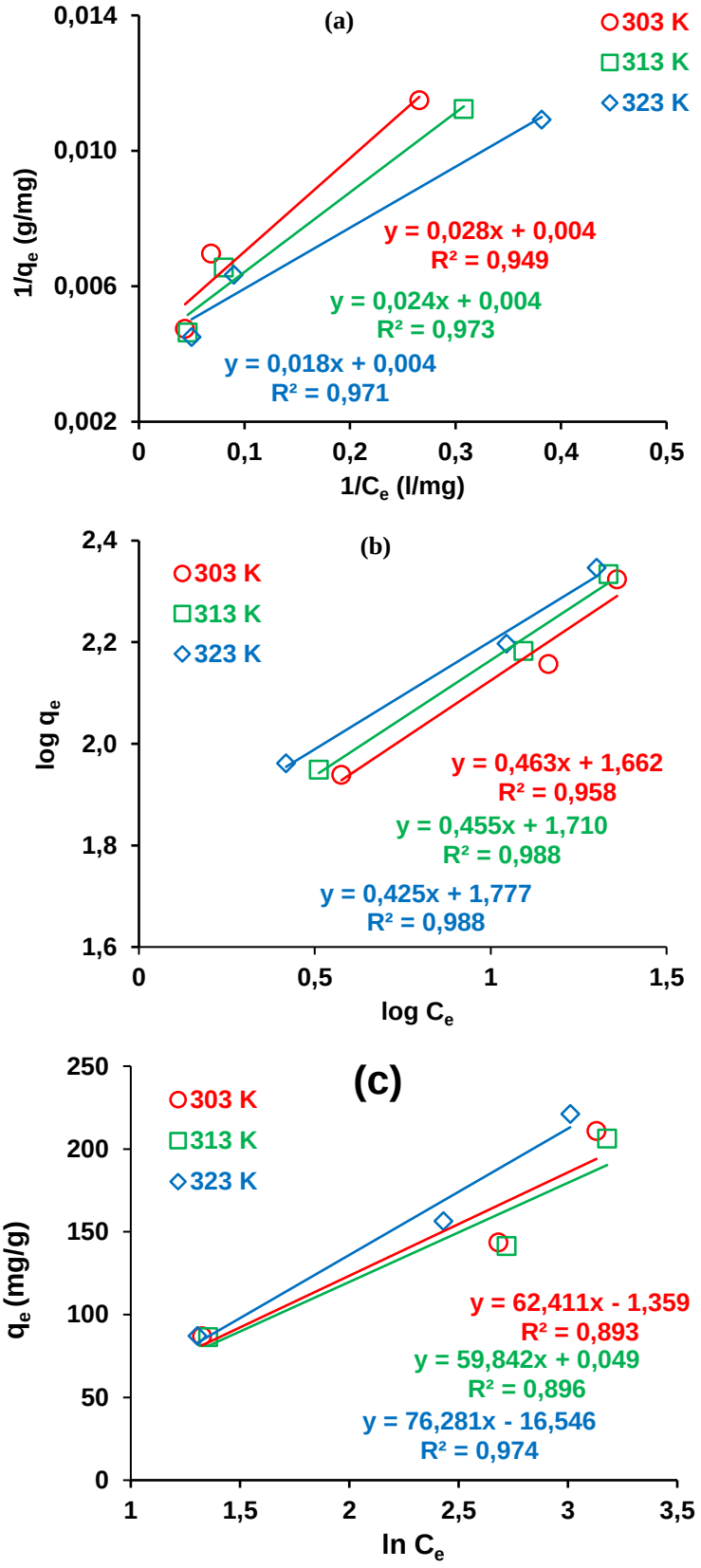

Fig. 10. Graphs of isotherm models for CR uptake onto F-SBA-15 (a) Langmuir, (b) Freundlich, and (c) Temkin ([CR]$_o$: 25–75 mg/l; pH: 7.9–8.2; Dosage: 0.25 g/l; Temp.: 303–323 K)

T a b l e 7

Constants and R^2 values calculated by isotherm models for CR uptake onto F-SBA-15 ($[CR]_o$: 25 – 75 mg/l; pH= 7.9 – 8.2; Dosage: 0.25 g/l; Temp.: 303 – 323 K)

T (K)	$Q_{max,exp}$	Langmuir				Freundlich			Temkin		
		Q_{max} (mg/g)	K_L (l/mg)	R^2	R_L	n	K_f (l/mg)	R^2	n	K_f (l/mg)	R^2
303	206.3	232.6	0.156	0.949	0.08–0.20	2.17	45.92	0.958	62.41	0.978	0.893
313	213.2	243.9	0.174	0.973	0.07–0.19	2.22	51.27	0.988	59.84	1.001	0.896
323	218.1	243.9	0.228	0.971	0.01–0.04	2.38	59.83	0.988	76.28	0.805	0.974

4. CONCLUSION

Pure SBA-15 silica was functionalized with a secondary amine functional group, trimethoxy[3-(methylamino)propyl] silane, to improve its ability for Congo Red (CR) adsorption. The synthesized material was characterized using small- and wide-angle XRD, N_2 adsorption-desorption isotherms, SEM, and TEM. Functionalization led to a reduction in BET surface area, pore volume, and pore diameter, attributable to the occupation of the surface by the modifier molecules. Characterization results revealed that the mesoporous structure of SBA-15 remained intact after functionalization; however, its order was diminished.

Kinetic studies showed that the CR adsorption process fits the PSO model, with a strong affinity for the modified SBA-15 surface. Temperature positively affected the uptake capacity and yield; thermodynamic coefficients indicated that the process was endothermic and non-spontaneous. The adsorption yield decreased with initial CR concentration but increased with the F-SBA-15 dosage. A maximum adsorption capacity of 211.1 mg/g was achieved with F-SBA-15, which was within the range of values reported in the literature for CR removal using various types of mesoporous adsorbents. The adsorption process agreed with the Freundlich isotherm, although the determination coefficients obtained with the Langmuir isotherm model were also high. This study shows that secondary amine-modified SBA-15 can be used for the removal of CR from aqueous media.

Acknowledgements. The study received no specific grant from any funding agency. The researchers would like to express their gratitude to Konya Technical University for providing the necessary resources.

Competing interests. Authors declare that they have no conflicting interests.

REFERENCES

(1) Liu, H.; Yu, H.; Jin, P.; Jiang, M.; Zhu, G.; Duan, Y.; Yang, Z.; Qiu, H., Preparation of mesoporous silica materials functionalized with various amino-ligands and investigation of adsorption performances on aromatic acids. *J. Chem. Eng.* **2020**, *379*, 122405.

(2) Yokoi, T.; Kubota, Y.; Tatsumi, T., Amino-functionalized mesoporous silica as base catalyst and adsorbent. *Appl. Catal. A-Gen.* **2012**, *421*, 14–37.

(3) Pamungkas, N. S.; Wongsawaeng, D.; Swantomo, D.; Kamonsuangkasem, K.; Chio-Srichan, S., Exploring qualitative and quantitative decoration on amine-modified mesoporous silica for enhance adsorption performances. *Eng. J.* **2023**, *27*, 45–55.

(4) Shen, J.; Zhang, S.; Zeng, Z.; Huang, J.; Shen, Y.; Guo, Y., Synthesis of magnetic short-channel mesoporous silica SBA-15 modified with a polypyrrole/polyaniline copolymer for the removal of mercury ions from aqueous solution. *ACS Omega* **2021**, *6*, 25791–25806.

(5) Mureseanu, M.; Reiss, A.; Stefanescu, I.; David, E.; Parvulescu, V.; Renard, G.; Hulea, V., Modified SBA-15 mesoporous silica for heavy metal ions remediation. *Chemosphere* **2008**, *73*, 1499–1504.

(6) Giraldo, L.; Moreno-Piraján, J. C., Study on the adsorption of heavy metal ions from aqueous solution on modified SBA-15. *Mater. Res.* **2013**, *16*, 745–754.

(7) Albayati, T. M.; Sabri, A. A.; Abed, D. B., Functionalized SBA-15 by amine group for removal of Ni(II) heavy metal ion in the batch adsorption system. *Desalin. Water Treat.* **2020**, *174*, 301–310.

(8) Liu, F.; Wang, A.; Xiang, M.; Hu, Q.; Hu, B., Effective adsorption and immobilization of Cr(VI) and U(VI) from aqueous solution by magnetic amine-functionalized SBA-15. *Sep. Purif. Technol.* **2022**, *282*, 120042.

(9) Masoudnia, S.; Juybari, M. H.; Mehrabian, R. Z.; Ebadi, M.; Kaveh, F., Efficient dye removal from wastewater by functionalized macromolecule chitosan-SBA-15 nanofibers for biological approaches. *Int. J. Biol. Macromol.* **2020**, *165*, 118–130.

(10) Zeidan, H.; Can, M.; Marti, M. E., Synthesis, characterization, and use of an amine-functionalized mesoporous silica SBA-15 for the removal of Congo Red from aqueous media. *Res. Chem. Intermed.* **2023**, *49*, 221–240.

(11) Gibson, L. T., Mesosilica materials and organic pollutant adsorption: Part A Removal from air. *Chem. Soc. Rev.* **2014**, *43*, 5163–5172.

(12) Yaghobi, N.; Hajiaghababaei, L.; Badiei, A.; Ganjali, M. R.; Mohammadi Ziarani, G., Controlled release of amoxicillin from bis(2-hydroxyethyl)amine functionalized SBA-15 as a mesoporous sieve carrier. *J. Chem. Health Risks* **2019**, *9*, 253–261.

(13) Uslu, H.; Marti, M., Equilibrium data on the reactive extraction of picric acid from dilute aqueous solutions using amberlite LA-2 in ketones. *J. Chem. Eng. Data* **2017**, *62*, 2132–2135

(14) Marti, M. E.; Zeidan, H., Evaluation of beet sugar processing carbonation sludge for the remediation of synthetic dyes from aqueous media. *Int. J. Environ. Sci. Technol.* **2023**, *20*, 3875–3890.

(15) Ariaeenejad, S.; Motamedi, E.; Salekdeh, G. H., Highly efficient removal of dyes from wastewater using nanocellulose from quinoa husk as a carrier for immobilization of laccase. *Bioresour. Technol.* **2022**, *349*, 126833.

(16) Sarfraz, S.; Ullah, H.; Sikandar, S.; Raza, A., Use of nano-sized adsorbents for wastewater treatment: a review. *Int. J. Econ. Environ. Geol.* **2022**, *13*, 23–29.

(17) Bilal, M.; Ihsanullah, I.; Shah, M. U. H.; Reddy, A. V. B.; Aminabhavi, T. M., Recent advances in the removal of dyes from wastewater using low-cost adsorbents. *J. Environ. Manage.* **2022**, *321*, 115981.

(18) Ali, K.; Zeidan H.; Amar, R. B., Evaluation of the use of agricultural waste materials as low-cost and eco-friendly sorbents to remove dyes from water: a review. *Desalin. Water Treat.* **2023**, *302*, 231–252.

(19) Salahshoor, Z.; Shahbazi, A., Modeling and optimization of cationic dye adsorption onto modified SBA-15 by application of response surface methodology. *Desalin. Water Treat.* **2016**, *57*, 13615–13631.

(20) Boukoussa, B.; Hakiki, A.; Moulai, S.; Chikh, K.; Kherroub, D. E.; Bouhadjar, L.; Guedal, D.; Messaoudi, K.; Mokhtar, F.; Hamacha, R., Adsorption behaviors of cationic and anionic dyes from aqueous solution on nanocomposite polypyrrole/SBA-15. *J. Mater. Sci.* **2018**, *53*, 7372–7386.

(21) Boukoussa, B.; Mokhtar, A.; El Guerdaoui, A.; Hachemaoui, M.; Ouachtak, H.; Abdelkrim, S.; Addi, A. A.; Babou, S., Boudina, B.; Bengueddach, A.; Hamacha, R., Adsorption behavior of cationic dye on mesoporous silica SBA-15 carried by calcium alginate beads: experimental and molecular dynamics study. *J. Mol. Liq.* **2021**, *333*, 115976.

(22) Abboud, M.; Sahlabji, T.; Haija, M. A.; El-Zahhar, A. A.; Bondock, S.; Ismail, I.; Keshk, S. M., Synthesis and characterization of lignosulfonate/amino-functionalized SBA-15 nanocomposites for the adsorption of methylene blue from wastewater. *New J. Chem.* **2020**, *44* (6), 2291–2302.

(23) Khan, A. J.; Song, J.; Ahmed, K.; Rahim, A.; Volpe, P. L. O.; Rehman, F., Mesoporous silica MCM-41, SBA-15 and derived bridged polysilsesquioxane SBA-PMDA for the selective removal of textile reactive dyes from wastewater. *J. Mol. Liq.* **2020**, *298*, 111957.

(24) Meechai, T.; Poonsawat, T.; Limchoowong, N.; Laksee, S.; Chumkaeo, P.; Tuanudom, R.; Yatsomboon, A.; Honghernsthit, L.; Somsook, E.; Sricharoen, P., One-pot synthesis of iron oxide-Gamma irradiated chitosan modified SBA-15 mesoporous silica for effective methylene blue dye removal. *Heliyon.* **2023**, 9.

(25) Siddiqui, S. I.; Allehyani, E. S.; Al-Harbi, S. A.; Hasan, Z.; Abomuti, M. A.; Rajor, H. K.; Oh, S., Investigation of Congo Red toxicity towards different living organisms: a review. *Processes.* **2023**, *11*, 807.

(26) Zhao, D.; Huo, Q.; Feng, J.; Chmelka, B. F.; Stucky, G. D., Nonionic triblock and star diblock copolymer and oligomeric surfactant syntheses of highly ordered, hydrothermally stable, mesoporous silica structures. *J. Am. Chem. Soc.* **1998**, *120*, 6024–6036.

(27) Bahalkeh, F.; Mehrabian, R. Z.; Ebadi, M., Removal of Brilliant Red dye (Brilliant Red E-4BA) from wastewater using novel Chitosan/SBA-15 nanofiber. *Int. J. Biol. Macromol.* **2020**, *164*, 818–825.

(28) Sujandi, Prasetyanto, E. A.; Park, S. E., Synthesis of short-channeled amino-functionalized SBA-15 and its beneficial applications in base-catalyzed reactions. *Appl. Catal. A-Gen.* **2008**, *350*, 244.

(29) Bhuyan, D.; Gogoi, A.; Saikia, M.; Saikia, R.; Saikia, L., Facile synthesis of gold nanoparticles on propylamine functionalized SBA-15 and effect of surface functionality of its enhanced bactericidal activity against gram positive bacteria. *Mater. Res. Express.* **2015**, *2*, 075402.

(30) Zhang, F.; Yang, C.; Li, Y.; Chen, M.; Hu, S.; Cheng, H., The preparation of organophosphorus ligand-modified SBA-15 for effective adsorption of Congo red and Reactive red 2. *RSC Adv.* **2019**, *9*, 13476–13485.

(31) Vandarkuzhali, S. A. A.; Pachamuthu, M. P.; Srinivasan, V. V.; Mohamed, S. K.; Abd Rabboh, H. S. M.; Hamdy, M. S.; Balamurugan, V. T., Efficient reduction of dyes to leuco form over silver nanoparticles on functionalised SBA-15 and aminoclay. *Int. J. Environ. Anal. Chem.* **2022**, *102*, 6359.

(32) Wang, X.; Lin, K. S. K.; Chan, J. C. C.; Cheng S., Direct synthesis and catalytic applications of ordered large pore aminopropyl-functionalized SBA-15 mesoporous materials. *J. Phys. Chem. B.* **2005**, *109*, 1763.

(33) Paul, L.; Mukherjee, S.; Chatterjee, S.; Bhaumik, A.; Das, D., Organically functionalized mesoporous SBA-15 type material bearing fluorescent sites for selective detection of Hg(II) from aqueous medium. *ACS Omega.* **2019**, *4*, 17857.

(34) Yang, Y.; Cao, X.; Ma, Z.; Wu, G.; Zheng, L.; Zhang, Y., Adsorption of Cu(II) and Cr(III) ions on SBA-15 mesoporous silica functionalized by branched amine. *Desalin. Water Treat.* **2021**, *213*, 358.

(35) Sadjadi, S.; Heravi, M. M.; Zadsirjan, V.; Farzaneh, V., SBA-15/hydrotalcite nanocomposite as an efficient support for the immobilization of heteropolyacid: A triply-hybrid catalyst for the synthesis of 2-amino-4H-pyrans in water. *Appl. Surf. Sci.* **2017**, *426*, 881.

(36) Albaker, R. I. B.; Kocaman, S.; Marti, M. E.; Ahmetli G., Application of various carboxylic acids modified walnut shell waste as natural filler epoxy-based composites. *J Appl. Polym. Sci*. **2021**, *138*, e50770

(37) Bhuyan, D.; Saikia, L., Scavenging Pd^{2+} on amine-functionalized SBA-15: A facile synthesis of leach-free Pd^{0} nanocatalyst for base-free Chemoselective Transfer Hydrogenation of Olefins. *ChemistrySelect.* **2017**, *2*, 6350.

(38) Hafezian, S. M.; Biparva, P., Bekhradnia, A.; Azizi, S. N., Amine and thiol functionalization of SBA-15 nanoparticles for highly efficient adsorption of sulforaphane. *Adv. Powder Technol.* **2021**, *32*, 779.

(39) Huang, C. H.; Chang, K. P.; Ou, H. D.; Chiang, Y. C.; Wang, C. F., Adsorption of cationic dyes onto mesoporous silica. *Micropor. Mesopor. Mat.* **2011**, *141*, 102.

(40) Zhu, Y.; Li, H.; Zheng, Q.; Xu, J.; Li, X., Amine-functionalized SBA-15 with uniform morphology and well-defined mesostructure for highly sensitive chemosensors to detect formaldehyde vapor. *Langmuir*. **2012**, *28*, 7843.

(41) Hakiki, A.; Boukoussa, B.; Zahmani, H. H.; Hamacha, R.; Abdelkader, N. H. H.; Bekkar, B.; Bettahar, F.; Nunes-Beltrao, A. P.; Hacini, S.; Bengueddach, A.; Azzouz, A., Synthesis and characterization of mesoporous silica SBA-15 functionalized by mono-, di-, and tri-amine and its catalytic behavior towards Michael addition. *Mater. Chem. Phys.* **2018**, *212*, 415.

(42) Siavashani, A. Z.; Nazarpak, M. H.; Fayyazbakhsh, F.; Toliyat, T.; McInnes, S. J. P.; Solati-Hashjin, M., Effect of amino-functionalization on insulin delivery and cell viability for two types of silica mesoporous structures. *J. Mater. Sci.* **2016**, *51*, 10897.

(43) Ahmed, K.; Rehman, F.; Pires Cleo, T. G. V. M. T.; Rahim, A.; Santos, A. L.; Airoldi, C., Aluminum doped mesoporous silica SBA-15 for the removal of remazol yellow dye from water. *Micropor. Mesopor. Mat.* **2016**, *236*, 167.

(44) Goscianska, J.; Olejnik, A.; Nowak, I., APTES-functionalized mesoporous silica as a vehicle for antipyrine – adsorption and release studies. *Colloids Surf. A: Physicochem. Eng. Aspects.* **2017**, *533*, 187.

(45) Liou, T. H.; Chen, G. W.; Yang, S., Preparation of amino-functionalized mesoporous SBA-15 nanoparticles and the improved adsorption of tannic acid in wastewater. *Nanomater.* **2022**, *12*, 791.

(46) Klimova, T.; Esquivel, A.; Reyes, J.; Rubio, M.; Bokhimi, X.; Aracil, J., Factorial design for the evaluation of the influence of synthesis parameters upon the textural and structural properties of SBA-15 ordered materials. *Micropor. Mesopor. Mat.* **2006**, *93*, 331.

(47) Ali, K.; Zeidan, H.; Marti, M. E., Evaluation of olive pomace for the separation of anionic dyes from aqueous solutions: kinetic, thermodynamic, and isotherm studies. *Desalin. Water Treat.* **2021**, *227*, 412–424.

(48) Lagergren, S., Zur Theorie der sogenannten adsorptiongeloster Stoffe. *Kungl. Svens. Vetenskapsakad.* **1898**, *24*, 1–39.

(49) Ho, Y. S.; McKay, G., Pseudo second order model for sorption process. *Process Biochem.* **1999**, *34*, 451–465.

(50) Elovich, S. Y.; Larinov, O., Theory of adsorption from solutions of non electrolytes on solid (I) equation adsorption from solutions and the analysis of its simplest form, (II) verification of the equation of adsorption isotherm from solutions. *Izv. Akad. Nauk. SSSR, Otd. Khim. Nauk.* **1962**, *2*, 209–216.

(51) Weber, W. J.; Morris, J. C., *Water Pollution Symposium. Proc. Int. Conf.* Pergamon Oxford., *2*, 231–266, 1962.

(52) Asim, H.; Zeidan, H.; Marti, M. E., Effective isolation of succinic acid from aqueous media with the use of anion exchange resins. *RSC Adv.* **2024**, *14*, 16765–16777.

(53) Sağlam, S.; Türk, F. N.; Arslanoğlu, H., Use and applications of metal-organic frameworks (MOF) in dye adsorption. *J. Environ. Chem. Eng.* **2023**, 110568.

(54) Zeidan, H.; Ozdemir, D.; Kose, N.; Pehlivan, E.; Ahmetli, G.; Marti, M. E., Separation of formic acid and acetic acid from aqueous solutions using sugar beet processing fly ash: characterization, kinetics, isotherms and thermodynamics. *Desalin. Water Treat.* **2020**, *202*, 283–294.

(55) Chen, S.; Zhang, J.; Zhang, C.; Yue, Q.; Li, Y.; Li, C., Equilibrium and kinetic studies of methyl orange and methyl violet adsorption on activated carbon derived from *Phragmites australis*. *Desalination* **2010**, *252*, 149–156.

(56) Annadurai, G.; Juang, R. S.; Lee, D. J., Use of cellulose-based wastes for adsorption of dyes from aqueous solutions. *J. Hazard. Mater.* **2002**, *92*, 263–274.

(57) Zeidan H.; Marti M. E., Efficient separation of levulinic acid using fly ash from sugar beet processing *Chem. Biochem. Eng. Q.* **2024**, *38*, 207–217.

(58) Lu, R.; Gan, W.; Wu, B. H.; Zhang, Z.; Guo, Y.; Wang, H. F., C−H stretching vibrations of methyl, methylene and methine groups at the vapor/alcohol (n = 1− 8) interfaces. *J. Phys. Chem. B.* **2005**, *109*, 14118–14129.

(59) Xia, C.; Jing, Y.; Jia, Y.; Yue, D.; Ma, J.; Yin, X., Adsorption properties of congo red from aqueous solution on modified hectorite: Kinetic and thermodynamic studies. *Desalination.* **2011**, *265*, 81–87.

(60) Chaudhuri, H.; Dash, S.; Sarkar, A., Synthesis and use of SBA-15 adsorbent for dye-loaded wastewater treatment. *J. Environ. Chem. Eng.* **2015**, *3*, 2866–2874.

(61) Abdelkader, E.; Nadjia, L.; Rose-Noëlle, V., Adsorption of Congo red azo dye on nanosized SnO_2 derived from sol-gel method. *Int. J. Ind. Chem.* **2016**, *7*, 53–70.

(62) Khalaf, I. H.; Al-Sudani, F. T.; AbdulRazak, A. A.; Aldahri, T.; Rohani, S., Optimization of Congo red dye adsorption from wastewater by a modified commercial zeolite catalyst using response surface modeling approach. *Water Sci. Technol.* **2021**, *83*, 1369–1383.

(63) Sholehah, F.; Taba, P.; Hala, Y.; Bahrun, B., Adsorption of congo red dyes using mesoporous silica MCM-48. *In: AIP Conference Proceedings (*Vol. 2360, No. 1). AIP Publishing. 2021.

(64) Pavan, F. A.; Dias, S. L.; Lima, E. C.; Benvenutti, E. V., Removal of Congo red from aqueous solution by anilinepropylsilica xerogel. *Dyes Pigm.* **2008**, *76*, 64–69.

(65) Langmuir, I., The constitution and fundamental properties of solids and liquids, Part I. Solids. *J. Am. Chem. Soc.* **1916**, *38*, 2221–2295.

(66) Freundlich, H.; Helle, W. J., Übber die Adsorption inlusungen. *J. Am. Chem. Soc.* **1939**, *61*, 2–28.

(67) Temkin, M. J.; Pyzhev, V. Recent modifications to Langmuir isotherms. *Acta Physicochim. USSR*. **1940**, *12*, 217–225.

(68) Ma, Y.; Qi, Y.; Yang, L.; Wu, L.; Li, P.; Gao, F.; Qi, X.; Zhang, Z., Adsorptive removal of imidacloprid by potassium hydroxide activated magnetic sugarcane bagasse biochar: Adsorption efficiency, mechanism and regeneration. *J. Clean. Prod.* **2021**, *292*, 126005.

(69) Can C. E., Zeidan, H.; Marti, M. E. Efficient recovery of itaconic acid using weak and strong anion Exchange resins from aqueous solutions. *Ind. Eng. Chem. Res.* **2024**, *63*, 5833−5844.

(70) Elhadj, M.; Samira, A.; Mohamed, T.; Djawad, F.; Asma, A.; Djamel, N., Removal of Basic Red 46 dye from aqueous solution by adsorption and photocatalysis: equilibrium, isotherms, kinetics, and thermodynamic studies. *Sep. Sci. Technol.* **2020**, *55*, 867–885.